ORIGINAL RESEARCH

Roles of Fatty Acid Chain Length and Enzyme-Oriented Drug Controlled Release from pH-Triggering Self-Assembled Fatty Acid Conjugated Quetiapine Nanosuspensions

Hy D Nguyen [1], Hai V Ngo [1], Van Hong Nguyen[2], Myung-Chul Gil [1,3], Beom-Jin Lee[1,4]

[1]College of Pharmacy, Ajou University, Suwon, 16499, Republic of Korea; [2]Department of Life Sciences, University of Science and Technology of Hanoi, Vietnam Academy of Science and Technology, Hanoi, 10000, Vietnam; [3]PLUTO Inc, Seongnam, 13453, Republic of Korea; [4]Institute of Pharmaceutical Science and Technology, Ajou University, Suwon, 16499, Republic of Korea

Correspondence: Beom-Jin Lee, College of Pharmacy, Ajou University, Suwon, 16499, Republic of Korea, Tel +82 31 219 3442, 3430, Fax +82 31 212 3653, Email bjl@ajou.ac.kr

Background: Quetiapine (QTP) is a first-line antipsychotic drug, but its therapeutic druggability and patient adherence were limited due to high oral dose strength, low bioavailability and physicochemical/biopharmaceutical issues.

Purpose: To investigate the roles of fatty acid chain length and enzyme-oriented QTP controlled release from pH-triggering self-assembled fatty acid conjugated QTP nanosuspensions (NSPs).

Methods: QTP was conjugated with different chain length fatty acids (C10–decanoic acid, C14–myristic acid, C18–stearic acid) to obtain QTP-fatty acid conjugates (QFCs: QD, QM, QS) by exploiting 1-ethyl-3-(3-dimethylaminopropyl) carbodiimide/4-dimethylaminopyridine (EDC/DMAP) conjugation chemistry. Then, the solubility, partitioning coefficient (log P), cell viability and cleavage kinetics of QFCs were evaluated. The pH-triggering self-assembled behaviors of QFCs to form QTP-fatty acid NSPs (QDN, QMN, QSN) by varying pH, QFC concentration and proton-to-QTP ratios were characterized. The morphological images, critical micelle concentration (CMC), physico-chemical properties and enzyme-oriented QTP controlled release of NSPs were examined.

Results: Three QFCs were synthesized with different chain length fatty acids from QTP after desalting fumarate from QTP fumarate. The pH, QFC concentration and proton-to-quetiapine molar ratio could influence physicochemical properties and nanonization behaviors of QFCs. All three QFCs showed no effect on the viability of myoblast cells. The pH-triggering self-assembly of amphiphilic QFCs to form nanoparticles (NPs) occurred as the amine moiety of QTP was readily ionized in a strongly acidic environment (pH 1.2). Interestingly, the longer the fatty acid chain length, the lower water solubility, the higher log P (lipophilicity) and the smaller NP particle size were observed. The conversion rate of QFCs to liberate QTP by esterase in human plasma and liver S9 fractions was also inversely proportional to the fatty acid carbon chain length. Interestingly, the freeze-dried QMN showed the esterase-oriented controlled release of QTP over one month, unlike the initial burst release of QDN or the slowly delayed release pattern of QSN.

Conclusion: A new pH-triggering self-assembled nanonization platform was developed using different chain length fatty acid conjugated QTP in low pH environment. By varying fatty acid chain length, the enzyme-oriented QTP controlled release dosage form was challenged to enhance the therapeutic effectiveness of QTP.

Keywords: quetiapine, fatty acid conjugated quetiapine, fatty acid chain length, fattigation platform, nanonization, pH-triggering self-assembly, enzyme-oriented controlled release, nanosuspension

Introduction

For patients with mental disorders who experience abnormal thinking and perception, non-adherence to medication regimens was reported to be as high as 72%.[1] The frequent self-administration of conventional oral dosage forms offers challenges for these patients. Under this viewpoint, long-acting injectable (LAI) formulations have been developed as alternatives for improving patient compliance and treatment effectiveness to aim at reducing dosing frequency. Additionally, the use of LAI

Graphical Abstract

Design and Properties of pH-Triggering Self-Assembled Fatty Acid Conjugated Quetiapine nanosuspensions
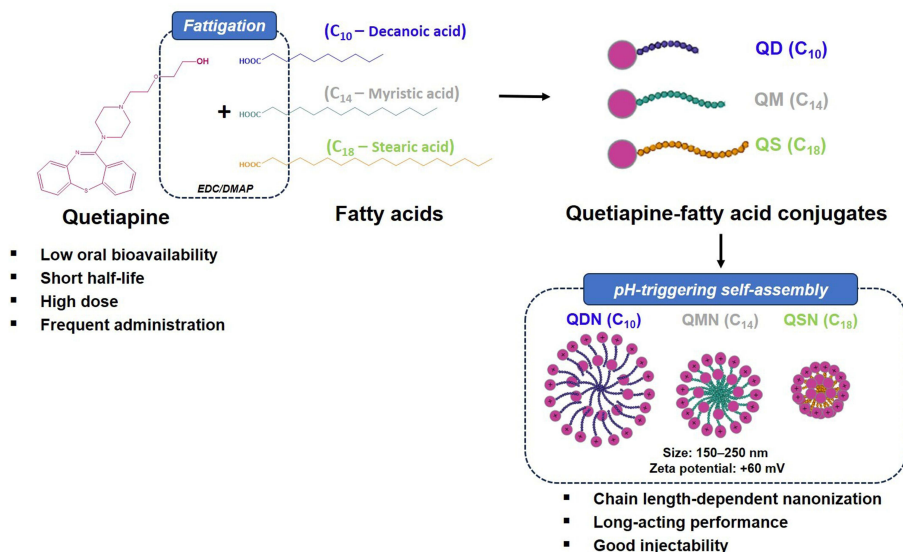
formulations can avoid absorption variability and first-pass metabolism, reducing the total dose and associated side effects as compared to oral dosage forms.[2,3] LAI formulations of antipsychotic drugs have been successfully formulated with a sustained release profile over several weeks intervals, such as oil-based solutions (haloperidol decanoate, flupentixol decanoate), microspheres (risperidone) and nanosuspensions (NSPs) (paliperidone palmitate, aripiprazole lauroxil).[4,5] Quetiapine (QTP) is one of the first-line antipsychotic drugs used to treat psychotic disorders, with fewer side effects and associated problems than other antipsychotic drugs.[6,7] However, this drug has low oral bioavailability (9%) and a short half-life (7 h) because of an extensive first-pass effect, requiring a high dose (150 to 800 mg per day) and frequent administration (once or twice a day).[6,8] Table 1 provides physicochemical and biopharmaceutical properties of QTP. These characteristics contributed to low patient adherence to QTP tablets, indicating the vital necessity for LAI formulations of QTP.

Among several types of LAI formulations, NSPs have been considered as one of the superior dosage forms. NSPs in water do not contain viscous oil or organic solvents like solution-based formulations that cause long-lasting pain or toxicity.[9] Compared to microsphere formulations with large particle sizes, NSPs offer better injectability with a faster

Table 1 Physicochemical and Biological Properties of Quetiapine (QTP) Fumarate

Factor	Quetiapine Fumarate
Physical appearance	White solid
Molecular weight	883.1 g/mol
Chemical formula	$(C_{21}H_{25}N_3O_2S)_2 \cdot C_4H_4O_4$
Solubility in water	0.5869 mg/L
Log P	2.81
Drug class	Atypical antipsychotics
Route of administration	Oral tablet (150–800 mg/day)
Half-life	6–7 h
Excretion	Liver
Oral bioavailability	9%

increase in plasma drug levels after administration.[2,10] However, the current preparation methods of NSPs require complicated pharmaceutical techniques for particle size reduction (wet milling or high-pressure homogenization) with the potential erosion of milling material.[11,12] Herein, we used a new approach of fattigation platform to develop LAI formulation of QTP. The fattigation platform has been launched by our research group as an innovative technique involving the chemical conjugation of biomacromolecules such as albumin, gelatin and peptide drugs with fatty acids to form amphiphilic structures. These structures could self-assemble in an aqueous solution, serving as drug nanocarriers or self-assembled prodrugs to improve the physicochemical properties and biopharmaceutical performance of drugs.[13–15] Upon conjugating the drug with long-chain fatty acids (palmitic acid, lauric acid), the obtained drug–fatty acid conjugates show low solubility in water and require enzymatic conversion to the active drug for therapeutic effect, which improved the drug half-life for LAI formulation.[2,16] The fattigation platform also offered a self-assembled ability to obtain nanoparticles (NPs) that can be injectable using a thin gauge needle and reduce the pain for patients.[14,15]

In this study, QTP-fatty acid conjugates (QFCs) by varying fatty acid chain lengths were synthesized and identified using various instrumental analyses. Then, the solubility, partitioning coefficient, cell viability and cleavage kinetics of QFCs were evaluated. The pH-triggering self-assembled behaviors of QFCs by varying pH, concentration and proton-to-QTP ratios were characterized. The morphological images, critical micelle concentration (CMC) and physicochemical properties of freeze-dried NSPs were investigated. Finally, enzyme-oriented QTP controlled release of NSPs was examined in phosphate-buffered saline (PBS) containing 5 U/mL esterase.

Materials and Methods

Materials

QTP fumarate (USP) was purchased from Aurobindo Pharma Company, India. Decanoic acid, myristic acid, stearic acid, 1-ethyl-3-(3-dimethylaminopropyl) carbodiimide hydrochloride (EDC HCl), and 4-dimethylaminopyridine (DMAP) were purchased from Sigma-Aldrich (St. Louise, MO, USA). A human plasma sample was kindly donated by Seoul Clinical Laboratories (Suwon, Korea), and human liver S9 fraction was purchased from Thermo Fisher Scientific (Seoul, Korea). Polysorbate 80 (Tween 80) and esterase from porcine liver (lyophilized powder, ≥15 units (U)/mg, solid) were purchased from Sigma-Aldrich. High-performance liquid chromatography (HPLC) grade solvents, including methanol (MeOH), acetonitrile (ACN), tetrahydrofuran (THF), ethyl acetate (EtAc), and n-hexanes were supplied by Samchundang (Seoul, Korea). Phosphate-buffered saline (PBS) tablets, Dulbecco's modified Eagle medium (DMEM), fetal bovine serum (FBS), and penicillin-streptomycin were purchased from Sigma-Aldrich. Other chemicals and reagents used in this study were of analytical grade.

Synthesis and Identification of QFCs

The QTP base was obtained by liquid–liquid extraction (EtAc/sodium bicarbonate saturated solution) from QTP fumarate.[17] QTP (EtAc phase) was dried under high vacuum to obtain a yellowish viscous oil as the starting material for QFC synthesis. A series of QFCs were synthesized by esterifying the hydroxyl group of QTP with three saturated fatty acids (C10, C14, and C18 carbons) to yield a fattigated QTP (quetiapine decanoate [QD], quetiapine myristate [QM], quetiapine stearate [QS], respectively). Specifically, QTP (1 equiv.) and fatty acid (1.1 equiv.) were dissolved in THF before adding EDC HCl (coupling agent, 1.5 equiv.) and DMAP (catalyst, 0.2 equiv.). Thin-layer chromatography was used to monitor the reaction with n-hexane:EtAc:MeOH (3:1:1) as the mobile phase. The mixture was then stirred at 20–30°C until no QTP was left. All resultant conjugates were purified by silica gel column chromatography using a mixture of EtAc and n-hexanes at 2:1 and 6:1 as an eluent. After drying under high vacuum to eliminate organic solvents, the purified QFCs were obtained as yellowish viscous oils.

The successful synthesis of QFCs was confirmed by Fourier-transform infrared (FT-IR) spectroscopy, proton and carbon-13 nuclear magnetic resonance (^{1}H and ^{13}C NMR), and matrix-assisted laser desorption/ionization time-of-flight mass spectroscopy (MALDI-TOF MS). FT-IR spectra were recorded over the range of 4000–400 cm^{-1} with a resolution of 4 cm^{-1} in a single scan (Nicolet iS50, Thermo Fisher Scientific). For ^{1}H NMR and ^{13}C NMR, chloroform-d was used as the solvent, and sample spectra were recorded using a Bruker Advance system operating at 400 MHz and 25°C. The

molecular mass was determined using MALDI-TOF/TOF MS on an Ultraflex III TOF/TOF mass spectrometer (Bruker Daltonics, Billerica, MA, USA).

Solubility and Log P of QTP Fumarate and QFCs

The partition coefficient (log P) values of QTP fumarate and the conjugates were calculated by determining their solubility in water and n-octanol. Briefly, an excess amount of each substance was added to the mixture of deionized water and n-octanol, mixed, and then kept stable at 25°C for 48 h. Samples were centrifuged at 10,000 rpm for 10 min using a CF-10 high-performance centrifuge (Wertheim, German) to achieve complete phase separation. For QTP fumarate, both aqueous and n-octanol supernatants were diluted with MeOH prior to analysis. For QD, QM, and QS, aqueous supernatants were frozen, lyophilized, and resuspended in MeOH, while n-octanol supernatants were prepared for analysis using direct dilution with MeOH.[18] Samples were analyzed for drug concentration using the HPLC-UV method. The experiments were performed in triplicate, and the average values were reported.

Cleavage Kinetics in Human Plasma and Human Liver Fractions

The cleavage kinetics of QD, QM, and QS and the release of QTP were determined in PBS, human plasma and human liver S9 fractions.[18,19] Briefly, 100 µL of QD, QM, and QS (10 mg/mL in DMSO) was incubated in 2 mL of PBS, human plasma or PBS containing human liver S9 fractions (1 mg/mL) at 37°C. At the specified time points, 100 µL of each sample was withdrawn and diluted with 1 mL of cold MeOH to stop the reaction. For the 0-min time point, 100 µL sample was withdrawn and mixed with cold MeOH immediately after adding the conjugates into the plasma or liver fraction. Samples were vortexed for 1 min, centrifuged at 10,000 rpm for 10 min, and the supernatants were analyzed for drug content using the HPLC-UV method. The experiments were performed in triplicate, and the average values were reported. The use of human plasma and human liver S9 fraction in this study was approved by the ethics committee of the Institutional Review Board, Ajou University (register number 2023-0126-001).

Quantification of QTP, QD, QM and QS Using HPLC-UV

The HPLC system (Agilent 1200, Agilent Technologies, USA) with an ultraviolet detector and Empower software was used to measure the drug concentrations. QTP, QD, QM, and QS were separated on a Hypersil gold 5 µm C18 column (250 × 4.6 mm) and detected at 230 nm using isocratic elution with a flow rate of 1.3 mL/min. The mobile phase for QTP quantification comprised 54% MeOH, 7% ACN, and 39% dibasic ammonium phosphate solution (2.6 g/L). The mobile phases for the three QFCs contained 0.1% trifluoroacetic acid in the mixture of ACN and water, with the ACN ratio of 60%, 70%, and 85% for QD, QM, and QS, respectively. The drug content was determined relative to the peak areas of drug standards (0.001–0.1 mg/mL) in MeOH.

Cell Viability of QFCs

Cell viability was assessed using the water-soluble tetrazolium salt (WST) assay kit (EZ-Cytox, Dogen, Korea).[20] Mouse myoblast cells (C2C12, ACTT) were plated in 96-well plates at a density of 2×10^4 cells/well in Dulbecco's modified Eagle medium (DMEM) with 10% (v/v) fetal bovine serum (FBS) and 100 U/mL penicillin G sodium and incubated for 24 h. The medium was then replaced with fresh medium containing QTP fumarate and three QFCs at different concentrations equivalent to 100–10,000 µg/L of QTP, obtained by 100-fold dilution of the DMSO solution containing drug/conjugates with DMEM. After incubating for 24 h, the medium was replaced with a fresh medium containing the WST-1 agent at a concentration of 10% and incubated for 2 h at 37°C. After a succinate-tetrazolium reductase reaction, the resulting formazan dye was measured at 450 nm on a BioTek Synergy H1MF Multi-Mode Microplate-Reader. Cell viability was calculated using the following equation:

$$\text{Cell viability } (\%) = \frac{At - Ab}{Ac - Ab} x100$$

where Ab: absorbance of blank (culture medium without cells), At: absorbance of test samples (culture medium and test solution), and Ac: absorbance of positive control (culture medium without the test solution).

Effect of pH and QFCs Concentration on Self-Assembly Behaviors

The pH-triggering self-assembly of QFCs was investigated in three pH buffer solutions (pH 1.2, 2.7, and 4.5) based on the acid dissociation constant (pKa) of QTP. In this experiment, the concentration of conjugates in each buffer solution was 10 mg/mL. Each QFC (QD, QM, and QS) was dissolved in a mixture of THF and pH buffer at a ratio (v/v) of 1:1. The mixtures were stirred in a hood (700 rpm) for 24 h to eliminate THF. To evaluate the effect of QFC concentration on their self-assembly, a similar experiment was carried out in pH 1.2 buffer solution with different concentrations of QM (1, 5, 10, 20, 37.5, 50, and 100 mg/mL).

Determination of Critical Micelle Concentration of QFCs at pH 1.2 Buffer Solution

The critical micelle concentration (CMC) was determined to investigate the pH-triggering micellization of QFCs in pH 1.2 buffer solution using the fluorescence probe technique with pyrene as the hydrophobic probe.[21] Briefly, pyrene was dissolved in acetone at 3×10^{-4} M and was then transferred to a series of vials to obtain a controlled concentration of 6×10^{-7} M. After heating at 60°C for acetone evaporation, different concentrations of the three conjugates in a solution at pH 1.2 buffer solution (0.001–5 mg/mL) were added to pyrene. The mixture was sonicated for 2 h to equilibrate pyrene and the micelles. A fluorescence spectrophotometer (Infinite M200, Tecan) was employed to obtain the fluorescence spectrum of samples. The excitation wavelength and temperature were controlled at 336 nm and 25°C, respectively. The emission spectrum of each sample was scanned from 350 to 400 nm. Then, the intensity ratio of the first (I1 = 374 nm) and the third (I3 = 386 nm) energy bands in the pyrene emission spectrum was calculated to determine the CMC of different QFCs at pH 1.2 buffer solution.

Preparation and Physicochemical Characterization of Nanosuspensions

Three QFCs (QD, QM, and QS) were weighed and dissolved in the mixture of THF and pH 1.2 buffer solution (1:1, v/v) at a final concentration of 45, 50, and 55 mg/mL, respectively, keeping the same proton-to-quetiapine ratio (mol/mol) of 0.75. The mixtures were stirred in a hood (700 rpm) for 24 h to eliminate THF and yield self-assembled NSPs (QDN, QMN, and QSN). The NSPs in pH 1.2 were mixed with 10% (w/v) mannitol (cryoprotectant agent), frozen at −80°C for 24 h, and freeze-dried for 48 h to obtain a powdered form for long-term storage. Prior to injection, the freeze-dried powders were reconstituted in deionized water to obtain injectable QFC NSPs.

The hydrodynamic diameter and polydispersity index (PDI) were determined by dynamic light scattering (DLS) using an ELSZ-2000 system (Otsuka Electronics, Osaka, Japan). Zeta potential was measured on the same instrument to provide information about the surface charge of NPs. All samples were diluted to a concentration of 1 mg/mL in deionized water and analyzed in triplicate. The morphology of nanosuspension powders was assessed using FE-SEM (JSM-7900F, JEOL, Akishima, Japan) at 5 kV. The NPs were fixed on carbon-coated copper grids and sputter-coated with a gold/palladium alloy before processing for imaging. For TEM analysis, the samples were negatively stained with 2% phosphotungstic acid (w/v) on 200 mesh carbon-coated copper grids. The excess sample was removed with filter paper, and the grids were subsequently dried overnight in a hood before processing for imaging using FE-TEM Tecnai-G2 F30 S-Twin (FEI, Austin, Texas, US), operating at 300 kV with 0.20 nm point resolution.

Enzyme-Oriented Release Kinetics of Nanosuspensions

An in vitro drug release study was performed in 0.01 M PBS, pH 7.4, containing 0.5% polysorbate 80 and 0.1% sodium azide using a dialysis method.[2,22] To mimic the in vivo conditions, 5 U/mL of esterase (from porcine liver) was added to the medium.[23,24] NSPs were accurately weighed, dissolved in 1 mL of PBS, and filled in a 3 mL dialysis tube (Pur-A-Lyzer™, molecular weight cut-off [MWCO] 3500 Da), which in turn was placed in a 50 mL tube containing 40 mL of the release medium. The tube was incubated at 37°C in a shaking bath at 100 rpm. At each time point, 200 µL of the medium was withdrawn, and 200 µL of fresh buffer was added. Samples were diluted in MeOH for simultaneous quantitative analysis of QFCs and QTP using the HPLC-UV method.

Physical Stability of Nanosuspensions During Storage

QDN, QMN, and QSN were diluted in MeOH to analyze the concentrations of QTP and QFCs using the HPLC-UV method. The physical stability of the NSPs was evaluated for both lyophilized and liquid states by measuring the particle

size and PDI using the DLS method. Freeze-dried powder samples were stored at 25°C for 1, 2, and 4 weeks, and reconstituted in the diluent prior to evaluation. For the liquid state, the average diameter and PDI of NSPs were monitored over 96 h at 25°C. A similar experiment was performed for samples in PBS containing 5% FBS at 37°C over 96 h to mimic biological conditions.[21] The experiments were performed in triplicate, and average values were reported.

Statistical Analysis

Statistical analysis of the data was performed using analysis of variance with SigmaPlot version 14.0 (Systat software, San Jose, CA, US). The differences between samples were considered significant if the p-value was less than 0.05 (*), 0.01(**) or 0.001(***). The data are presented as mean ± standard deviation.

Results and Discussion

Synthesis and Identification of QFCs

To avoid the unwanted formation of fumarate ester by-products (QTP-fumaric acid conjugate), the fumarate anion was eliminated using liquid–liquid extraction before fattigation process. After neutralizing QTP fumarate in sodium bicarbonate solution, the obtained QTP base was soluble in the EtAc phase. The successful transformation from QTP fumarate salt to QTP was confirmed using ^{1}H-NMR (Figure S1). Thereafter, QTP base was then chemically modified by attaching the fatty acids with different carbon chain lengths, decanoic (C10), myristic (C14), and stearic (C18) acids, to yield three QFCs, including QD, QM, and QS, respectively. Figure 1 gives the stepwise synthetic process of three QFCs with different chain length fatty acids after desalting fumarate from QTP fumarate. Figure S2 shows the physical forms of QTP base and three QFCs at 20°C.

Instrumental analysis using FT-IR spectroscopy, MALDI-TOF MS, as well as ^{1}H and ^{13}C NMR spectroscopy were used to identify the chemical structure of the conjugates (Figure 2). The FT-IR spectra (Figure 2A) of QD, QM, and QS clearly showed the disappearance of a broad peak at approximately 3000–3500 cm^{-1} (-OH stretching), indicating the complete reaction of QTP. In the spectra of QFCs, two strong adsorption bands at 2850–3000 (-CH$_2$ stretch) and 1720–1740 cm^{-1} (C=O stretch) were observed, corresponding to the aliphatic carbon chain and ester group, respectively. The proton and carbon NMR spectra were also characterized in Figure 2B. Proton NMR spectra showed a triplet signal of 4.19–4.22 ppm and a multiplet signal of 1.21–1.31 ppm corresponding to the methylene ester (CH_2-OCO) and methylene groups of saturated chain of fatty acids (-CH_2-), respectively. Further, C$_\alpha$ and the terminal methyl group of fatty acids were identified as triplets at 2.28–2.32 and 0.86–0.90 ppm, respectively. Similarly, the appearance of multiple signals between 14.24 and 35.00 ppm in ^{13}C NMR spectra indicated the carbon atoms of the conjugated aliphatic chain. The successful reaction and purity of the conjugates were also confirmed by the peaks shifting from 166.3 ppm (COOH) to 173.8 ppm (COOR) in ^{13}C NMR spectra. MALDI-TOF MS affirmed the molecular weight of each QFC (Figure 2C). All QFCs were produced with approximately 75–85% chemical yields. The detailed explanation of NMR spectra and MALDI-TOF MS data of QTP fumarate and three QFCs were given in the Supporting Information, Part 1 Instrumental Characterization of QTP Fumarate and QFCs.
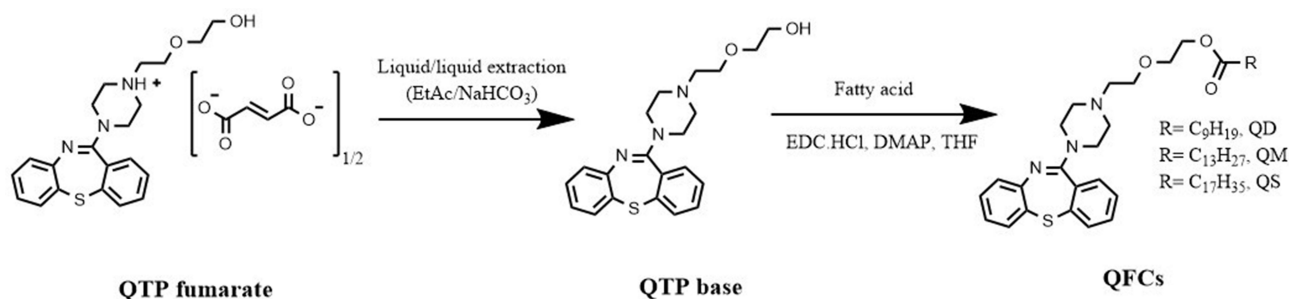

Figure 1 Stepwise synthetic process of three quetiapine-fatty acid conjugates with different fatty acid chain length from quetiapine fumarate.
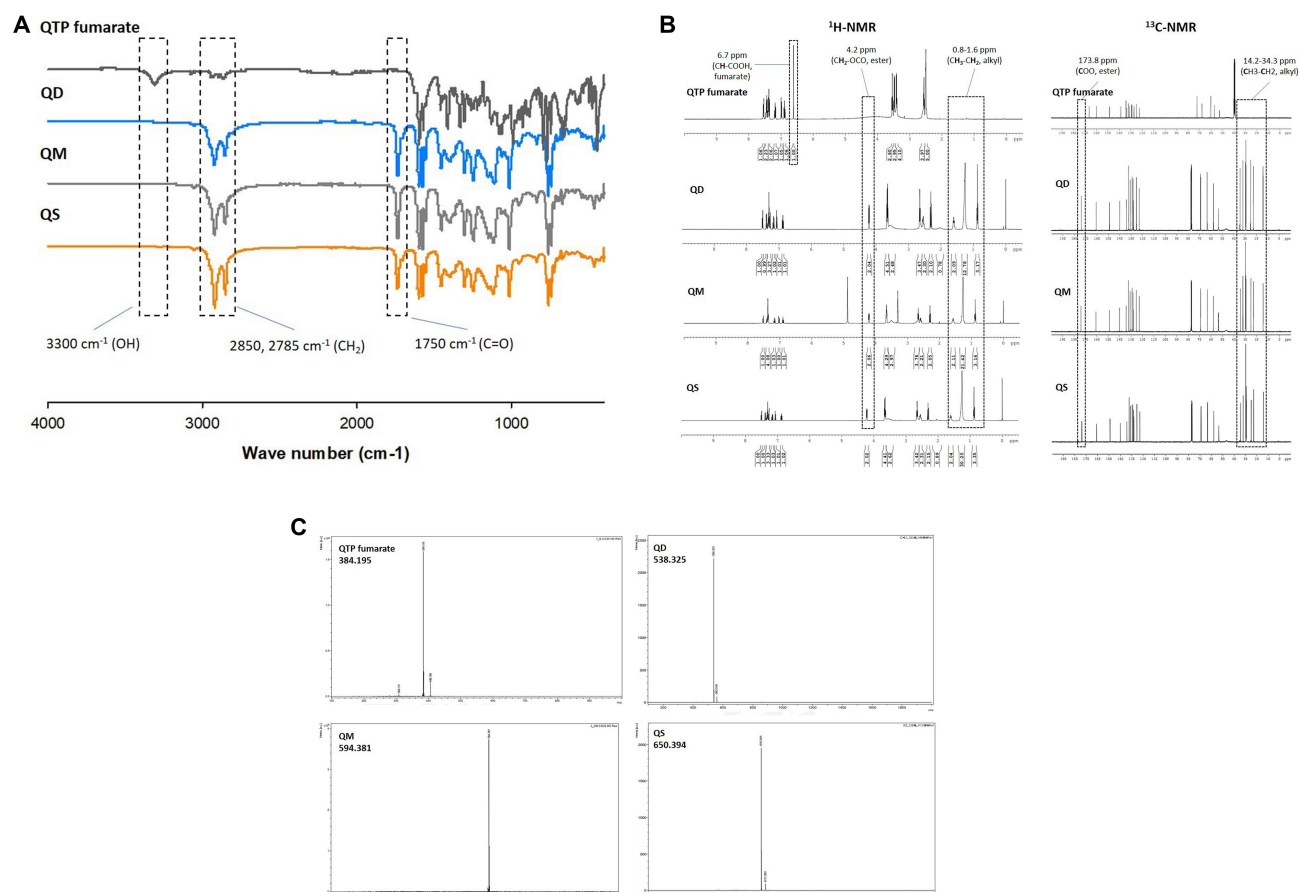
Figure 2 Identification of three quetiapine-fatty acid conjugates using instrumental analysis. (**A**) FT-IR spectroscopy, (**B**) ^{1}H and ^{13}C NMR spectroscopy and (**C**) MALDI-TOF-MS.

Physicochemical Properties of QFCs
Solubility and Log P of QTP Fumarate and QFCs

Solubility and log P of QTP fumarate and three QFCs in water and n-octanol were compared in Table 2. All QFCs were getting more lipophilic than QTP fumarate after fatty acid conjugation, resulting in higher solubility in n-octanol and lower solubility in water. Owing to the enhanced hydrophobicity and lipophilicity of QFCs as the chain length of fatty acid increased, the Log P values of QD, QM, and QS were gradually increased to 5.39 ± 0.06, 6.13 ± 0.12, and 7.00 ± 0.19, respectively, which were much higher than those of QTP fumarate (0.80 ± 0.04). The increased log P value was considered as one of the controllable physicochemical parameters of a drug candidate for long-acting and sustained release formulations, indicating the slow dissolution and enhanced half-life of the drug.[2]

Table 2 Solubility and Log P of QTP Fumarate and Three Quetiapine-Fatty Acid Conjugates (QFCs) in Water and n-Octanol (n = 3)

Substances	Solubility in Water (μg/mL)	Solubility in Octanol (mg/mL)	Log P
QTP fumarate	3533.92 ± 86.59	22.11 ± 1.75	0.80 ± 0.04
QD	1.90 ± 0.19	468.68 ± 43.63	5.39 ± 0.06
QM	0.45 ± 0.26	538.20 ± 11.04	6.13 ± 0.16
QS	0.07 ± 0.03	663.12 ± 7.85	7.00 ± 0.19

Cleavage Kinetics of QFCs to Convert QTP

Drug-fatty acid conjugates are pharmacologically inactive prodrugs that require enzymatic or hydrolytic conversion to the active QTP in physiological conditions for exerting therapeutic effects.[2] Therefore, the hydrolysis cleavage kinetics of QD, QM, and QS subsequently to convert QTP was evaluated in human plasma and the human liver S9 fraction, respectively in Figure 3. Owing to their extremely low solubility in water, all three conjugates were stable in PBS (pH 7.4) at 37°C for 1 month because no detection of the converted QTP was measured. In human plasma (Figure 3A), the conversion rate was proportional to the fatty acid chain length. QD was rapidly converted to QTP within 24 h, while QS was highly stable in human plasma for over 1 month with less than 10% QTP conversion. The medium-chain length QM showed gradual conversion to QTP over 1 month, with approximately 50% of QM cleaved after 7 days. A similar trend was observed in human liver extract, with approximately 100%, 50%, and 20% of three QD, QM, and QS conjugates, respectively, converted to QTP after 6 h (Figure 3B). It is known that esterases in the blood, intestine, and liver can play important roles in drug metabolism and detoxication by hydrolytic activities, showing species and organ tissue difference.[23,24] The different conversion rates of the same substance within the two microenvironments were explained by the higher esterase activity of the liver extract as compared to human plasma. These results indicate that the choice of fatty acid types is highly important in designing the drug-fatty acid conjugate for long-acting formulations via self-assembly. The cleavage kinetics of the drug-fatty acid conjugate and its half-life could thus be very crucial and manipulated by modifying the fatty acid carbon chain length.

Cell Viability of QFCs

In vitro viability of myoblast cells of QTP fumarate and three QFCs at various concentrations was investigated in Figure 4. At the concentration of 5000 μg/L or below, which was 50 times higher than the therapeutic dose of QTP (100 μg/L),[25] all three QFCs showed no effect on the viability of myoblast cells. At a concentration 100 times higher than
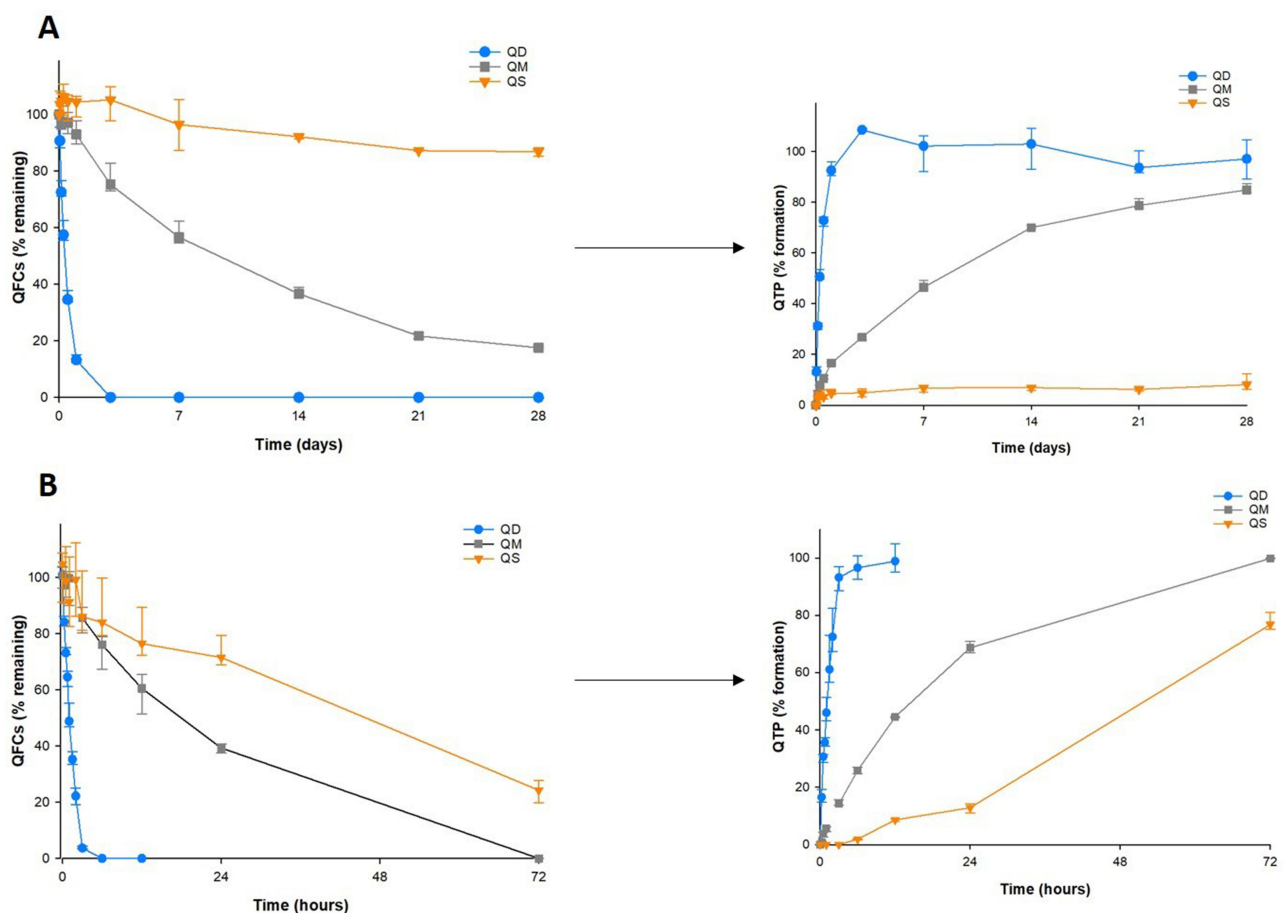

Figure 3 Conversion from quetiapine-fatty acid conjugates to quetiapine in human plasma (**A**) and liver fractions (**B**) (n=3).

the therapeutic dose (10,000 µg/L), all three conjugates were slightly more toxic to myoblast cells than QTP fumarate (88% compared to 98%). However, cell viability was still very high (almost 90%), with no significant difference among QD, QM, and QS, indicating the relative safety of these substances when injected into muscular tissues. This result also demonstrated that fatty acids were safe materials and that the carbon chain length had no effect on the toxicity of the conjugates.

Self-Assembly Behaviors of QFCs
Effect of pH and QFC Concentration

QTP has two amine groups in its chemical structure, which can be protonated with pKa values of 2.7 and 7.5. Therefore, it exhibits a pH-dependent solubility profile over a pH range of 1 to 7.5, with the maximal solubility observed at acidic pH (>80 mg/mL, pH 1.0) and minimal solubility (0.4 mg/mL) at pH 7.5 owing to the ionization to increase the drug hydrophilicity. The amphiphilicity of QFCs having a polar water-soluble QTP amine group attached to a water-insoluble fatty acid hydrocarbon chain was achieved.[26] Based on this chemical principle, the effect of pH and QFC concentration on the pH-triggering self-assembly behaviors of QFCs was investigated in Figure 5. The low pH acidic conditions, pH 1.2, 2.7, and 4.5 buffer solutions, were tested based on the pKa of QTP. Phase separation or aggregation was observed for all QFCs in pH 2.7 and 4.5 (Figure 5A). In contrast, QD, QM, and QS could self-assemble in low pH 1.2 buffer solution to obtain the respective NP systems with particle sizes varied depending on the fatty acid chain length (Table S1). These findings revealed that the amine moiety of QTP in the QFCs was readily ionized in a strongly acidic environment and subsequently self-assembled to form a NP system. This interesting process was entitled "pH-triggering self-assembly of QFCs" in this study.
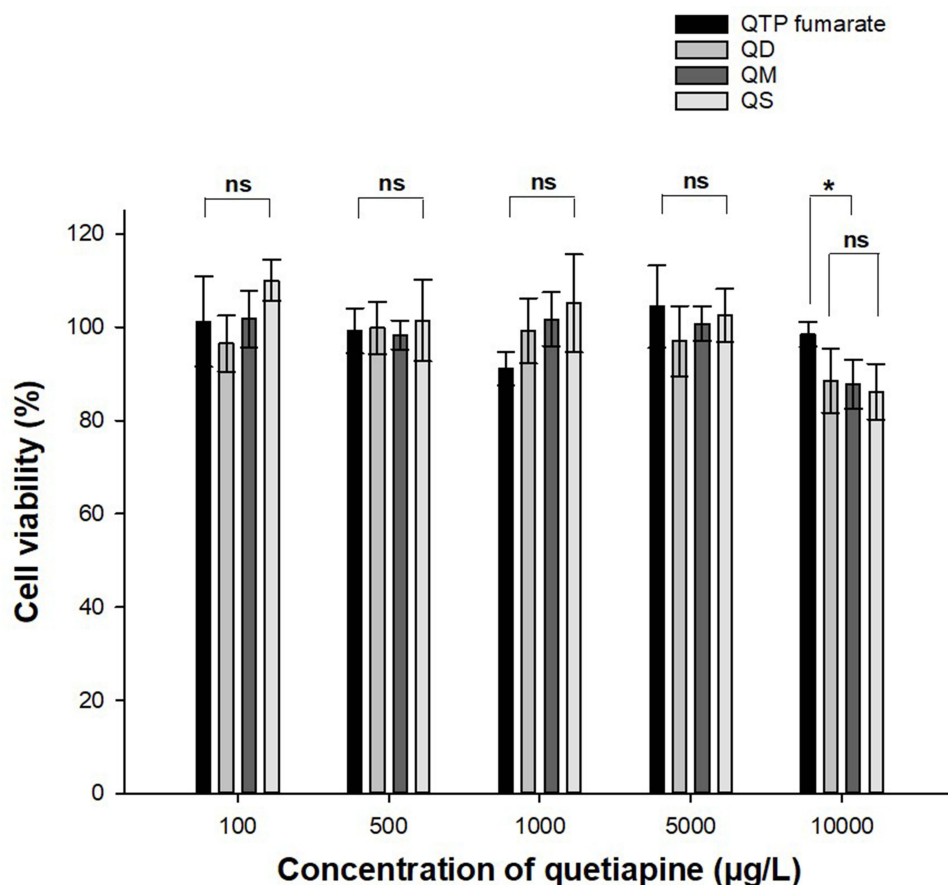

Figure 4 Cell viability of quetiapine fumarate and three quetiapine-fatty acid conjugates (n=4). The significant difference was analyzed by one-way ANOVA test (*p<0.05, ns: no significant difference).
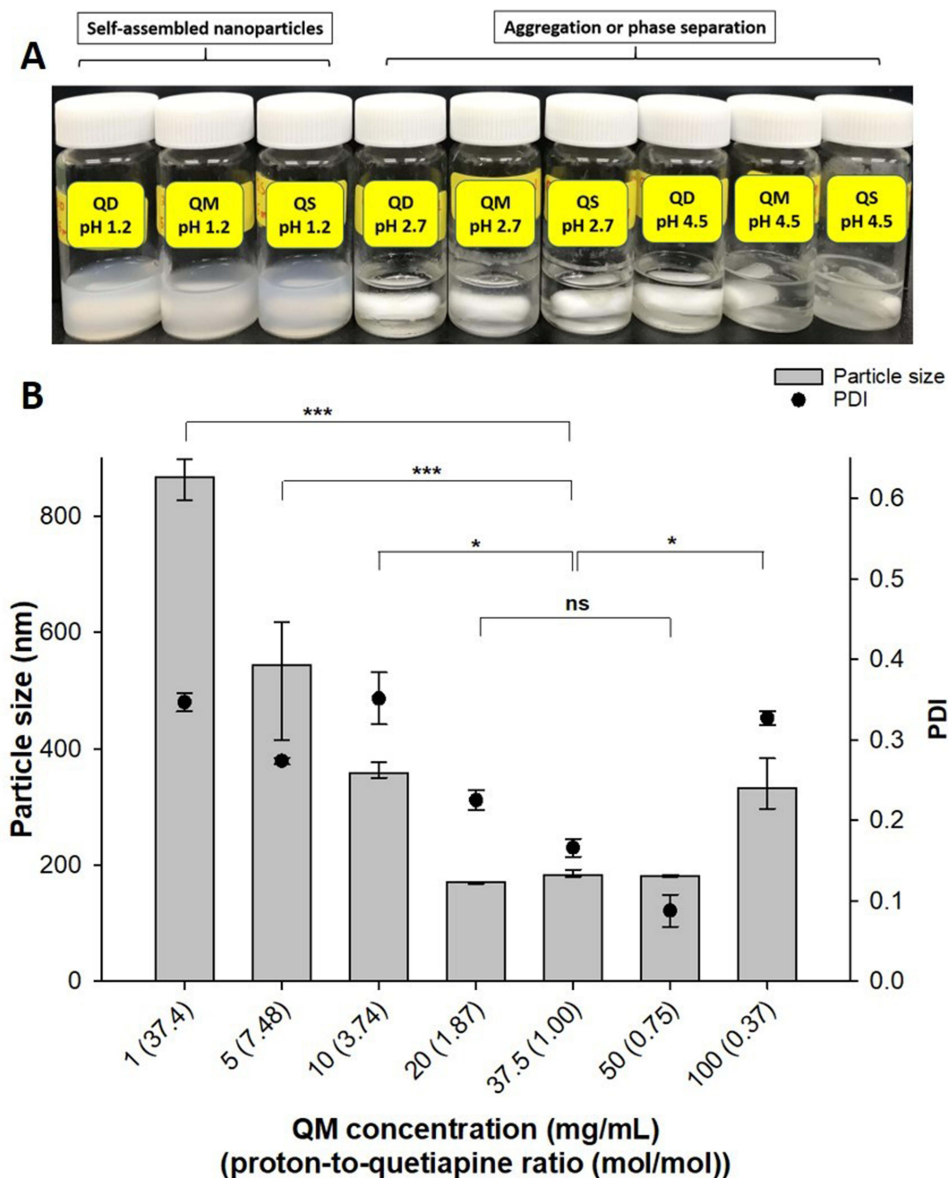
Figure 5 Effect of pH (**A**) and conjugate concentration (**B**) on the pH-triggering self-assembly behaviors of quetiapine-fatty acid conjugates. The significant difference was analyzed by one-way ANOVA test (***$p < 0.001$, *$p < 0.05$, ns: no significant difference).

The medium chain length conjugate (QM) was chosen to evaluate the effect of conjugate concentration on self-assembly behaviors at pH 1.2 buffer solution (Figure 5B). In the strongly acidic environment of pH 1.2, the percentage of QM molecules being ionized correlated with the ratio (mol/mol) between protons (H+) and QTP (proton-to-quetiapine ratio). At a high QM concentration of 100 mg/mL (proton-to-quetiapine ratio = 0.37), most QM molecules existed in a neutral form, and the NPs had wide particle size distribution (PDI > 0.3). Upon reducing the QM concentration to 50, 37.5, and 20 mg/mL corresponding to the proton-to-quetiapine ratios of 1.87, 1, and 0.75, respectively, more stable and smaller NPs of approximately 180 nm were created with no significant difference between the three concentrations. On the contrary, when the QM concentration was much lower than that of protons or the proton-to-quetiapine ratio (mol/mol) was much higher, the particle size was highly increased with a decrease in QM concentration owing to the aggregation of NPs. The aggregation can be explained by the electrostatic repulsion of excess protons (salting-out effect).[27] Together with pH, the proton-to-quetiapine ratio (mol/mol) was critical in preparing pH-triggering self-assembled NPs of QFCs. It appeared that a proton-to-quetiapine molar ratio of approximately 0.5–2 could give stable and small NPs. However,

particle-size distribution was narrower for the ratio of 0.75 (partial ionization) compared with that for 1 or 1.87 (complete ionization). Therefore, the proton-to-quetiapine molar ratio of 0.75 was chosen to prepare the self-assembled NPs of QFCs. If QFCs are fully ionized, the obtained NPs have a micelle structure. However, in the case of partial ionization, unionized QFCs could be readily packed inside the core of NPs to obtain the self-assembled NSPs (QDN, QMN and QSN).

Critical Micelle Concentration of QFCs at pH 1.2 Buffer Solution

Due to the low solubility and the lack of amphiphilicity, the QFCs were unable to form self-assembled NPs. However, pH-triggering nanonization of QFCs occurred in low pH condition owing to the ionization of amine groups of QTP to impart amphiphilicity of QFCs. Critical micelle concentration (CMC) of three QFCs to form pH-triggering self-assembled NPs in pH 1.2 buffer solution was determined in Figure 6. The CMC of QD, QM, and QS at pH 1.2 buffer solution was 0.6860, 0.1175, and 0.0469 mg/mL, respectively. These values were similar to the CMC of cationic surfactants with similar chemical structures, such as cetrimonium bromide or cetylpyridinium chloride (0.3–1 mg/mL), demonstrating the amphiphilic structure of QFCs at pH 1.2 buffer solution.[28,29] Moreover, the CMC values decreased following the order of QD, QM, and QS, revealing that QFCs with a longer fatty acid chain length giving higher lipophilicity were aggregated more easily to form micelles at the lower concentration. This finding was in agreement with previous studies showing that the CMC of amphiphilic molecules decreased with increasing carbon chain length.[29]

Physicochemical Properties and Enzyme-Oriented Controlled Release of Nanosuspension

Physicochemical Characterization of Nanosuspensions

Physicochemical properties of pH-triggering self-assembled NSPs of three QFCs were characterized in Table 3. The final concentration of QD, QM and QS was 45, 50, and 55 mg/mL, respectively, keeping the same proton-to-quetiapine ratio (mol/mol) of 0.75 in pH 1.2 buffer solution. The diameter of NPs was inversely proportional to the fatty acid carbon chain length, with average diameters of approximately 250, 180, and 150 nm for QDN, QMN and QSN, respectively. The longer the fatty acid chain length, the stronger was the hydrophobic interaction within the cores of self-assembled NPs.[30] The more lipophilic QS with a longer fatty acid chain length, the easier it is to form NPs with a smaller particle size of QSN as compared to QMN and QDN. Figure 7 shows the morphological images of NSPs using SEM and TEM, respectively. Based on the surface morphology of nanosuspension by detecting reflected or knocked-off electrons, the three NSPs, QDN, QMN and QSN, were distributed evenly with globular shapes and smooth surfaces. TEM images created by transmitted electrons passing through the nanosuspension showed that the NPs had a round, spherical particle shape. Additionally, in the case of QDN, a round membrane shape could be observed due to the charged polarity of QTP, but this was unclear in QMN and QSN as the NP size became smaller. It was also observed that longer fatty acid chain resulted in smaller particle sizes of NPs, with the order QDN > QMN > QSN, as discussed previously.
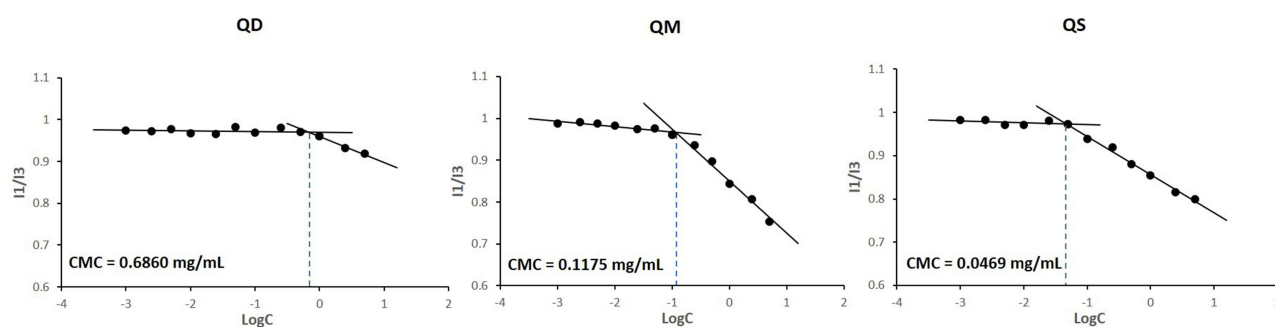

Figure 6 Critical micelle concentration (CMC) of three quetiapine-fatty acid conjugates to form pH-triggering self-assembled nanoparticles in pH 1.2 buffer solution.

Table 3 Physicochemical Properties of pH-Triggering Self-Assembled Nanosuspensions of Three Quetiapine-Fatty Acid Conjugates (QFCs)* (n = 3)

NSPs	Size (nm)	PDI	Zeta Potential (mV)
QDN	245.43 ± 7.09	0.19 ± 0.06	62.65 ± 4.31
QMN	177.73 ± 1.92	0.10 ± 0.02	59.57 ± 0.99
QSN	146.70 ± 2.46	0.26 ± 0.01	58.65 ± 3.93

Notes: *The final concentration of QD, QM and QS was 45, 50, and 55 mg/mL, respectively, keeping the same proton-to-quetiapine ratio (mol/mol) of 0.75.

Physical Stability of Nanosuspensions

The QD, QM, and QS must be stable in pH 1.2 buffer during the pH-triggering self-assembly with a negligible amount of conjugate hydrolyzed to QTP. In a preliminary experiment, the degradation ratios of three QFCs after pH-triggering self-assembly process were checked in Table S2. Compared with the initial concentration of conjugates, the hydrolysis rates for QDN, QMD, and QSN were 0.379%, 0.048%, and 0.015%, respectively.

The pH-triggering self-assembled NSPs at pH 1.2 buffer solution were freeze-dried to obtain a preferable solid state and provide long-term stability during storage. Figure 8 shows the changes in particle size and PDI of freeze-dried nanosuspension powder during storage for 4 weeks. The solid powder state of all QDN, QMN, and QSN was stable over 4 weeks under the storage condition with a minimal change in the particle size and PDI (Figure 8A). In the liquid state, QMN and QSN were also stable at 25°C, whereas the particle size of QDN gradually increased from approximately 250
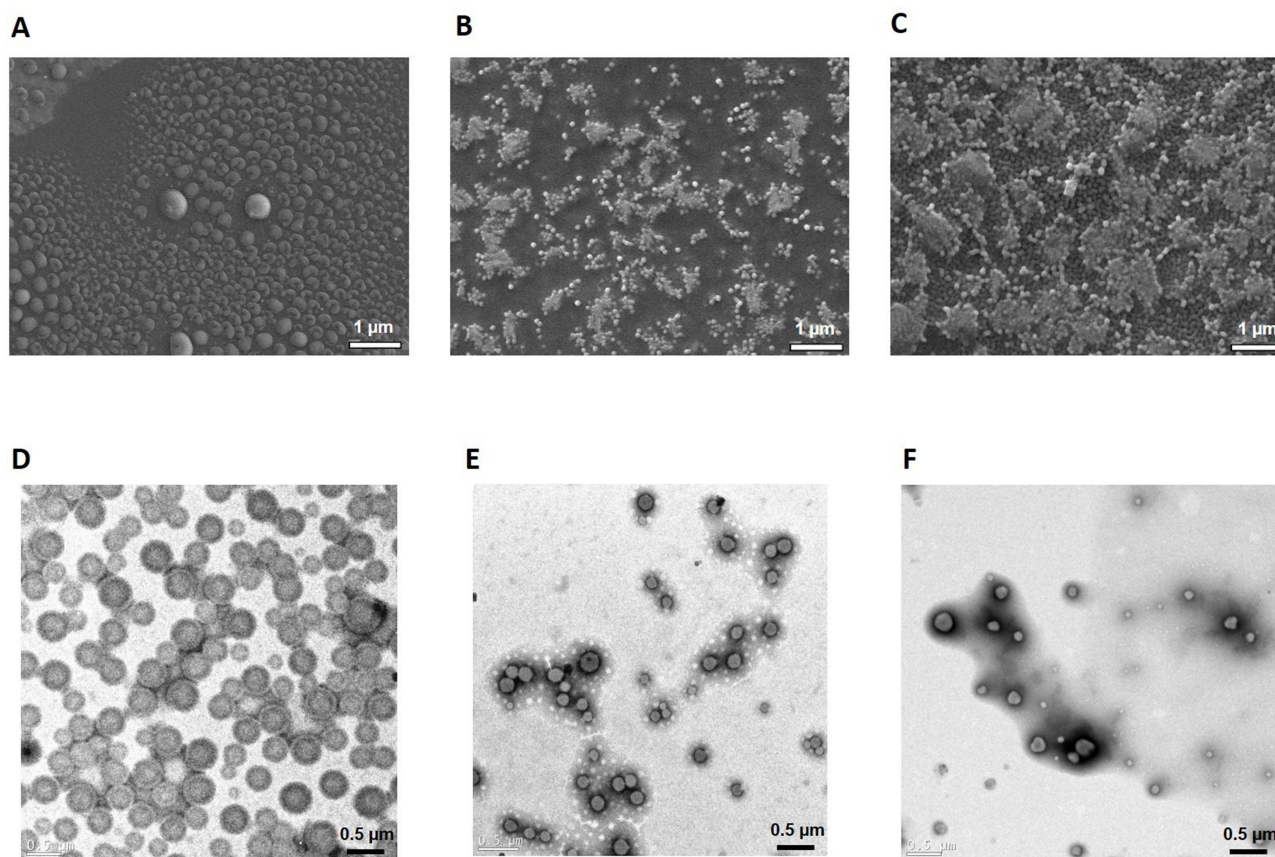

Figure 7 SEM (above) and TEM (below) images of pH-triggering self-assembled QDN (**A** and **D**), QMN (**B** and **E**) and QSN (**C** and **F**).
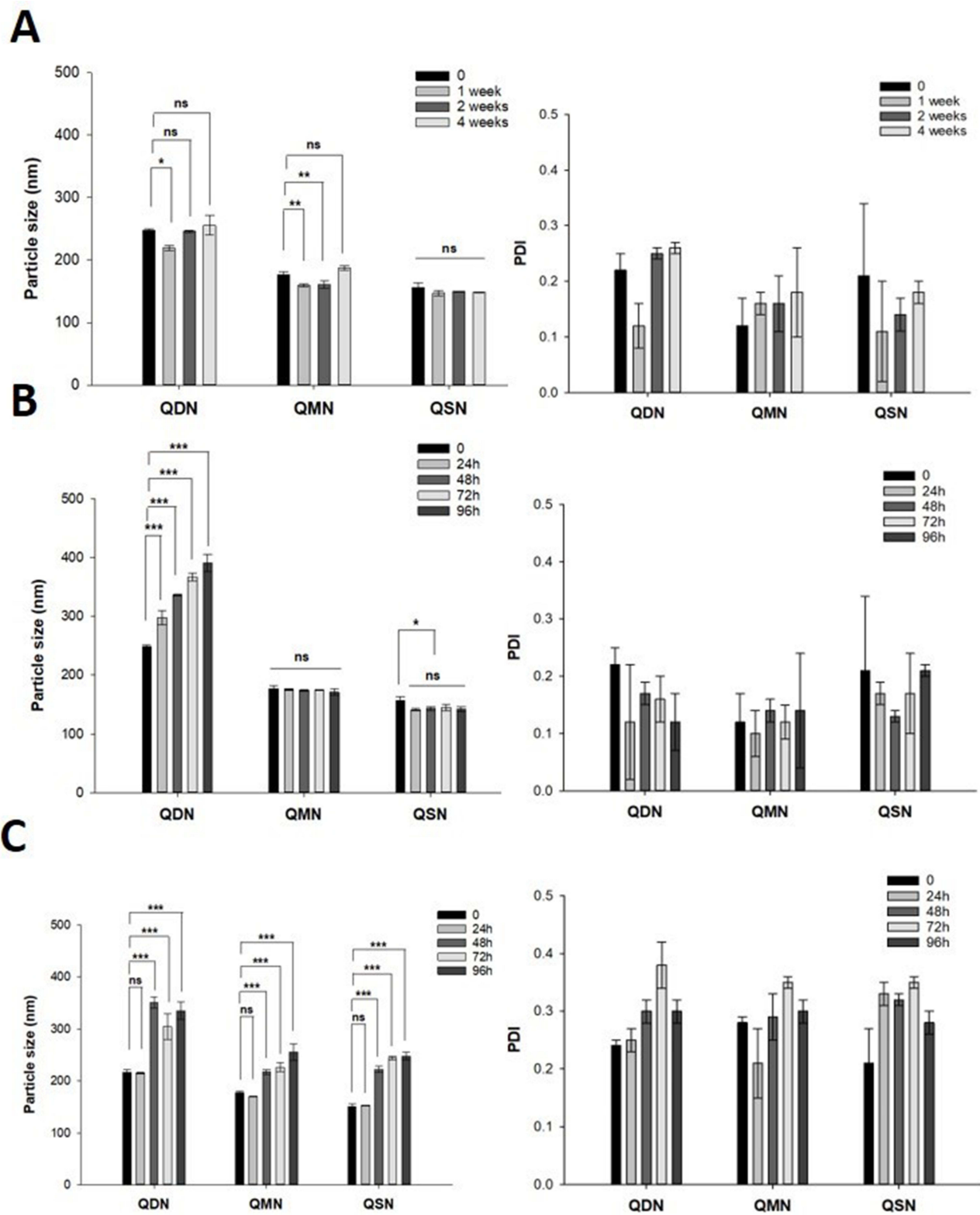
Figure 8 The changes of particle size and polydispersity index (PDI) of freeze-dried nanosuspension powder during storage for 4 weeks in solid state at 25 °C (**A**), liquid state at 25 °C (**B**) and 5% FBS/PBS at 37 °C (**C**) (n=3). The significant difference was analyzed by one-way ANOVA test (***p<0.001, **p<0.01, *p<0.05, ns: no significant difference).

to 400 nm over 96 h (Figure 8B). Owing to the weak hydrophobic interaction inside the core of NPs, QDN might be disassembled in an aqueous environment, leading to the increase in the particle size over time.

In 5% FBS/PBS at 37°C, all NSPs showed an increase in particle size after 48 h with wide distribution (PDI > 0.3) (Figure 8C). This instability might be explained by the conversion from NPs to QFCs in neutral pH, the enzymatic hydrolysis of the conjugates to QTP by esterase presented in FBS, or the adsorption of the proteins and substances to form protein corona. However, the dynamical stability of nanosuspension should be more important for therapeutic reasons. In other words, the solid-state nanosuspension must be stable during storage, but it should be dissembled to convert the conjugate and finally release QTP under physiological condition after intramuscular injection.

Enzyme-Oriented Controlled Release of Nanosuspensions

The QTP release from NSPs in the dialysis tube was hypothesized through two simultaneous steps. The first step was associated with the release of the conjugate from self-assembled NSPs, depending on the solubility of QFCs in the release media. In the second step, the conjugate was converted to QTP by esterase (5 U/L) contained in the media. Owing to its commercial availability, esterase from the porcine liver with high activity was used. The dialysis tube with a small MWCO of 3500 Da was used to retain NSPs inside the tube without interacting with the porcine esterase (MW of 168 kDa) in the release media. When QD, QM, and QS were rapidly converted to QTP by the porcine esterase, the concentration of conjugates in the release media would be maintained at a low level, and drug release could not be affected by the poor intrinsic solubility of lipophilic conjugates. For sink condition in release media, polysorbate 80 0.5% was added to improve the solubility of QFCs and QTP in PBS, whereas sodium azide served as an anti-microbial agent.

Figure 9 shows the enzyme-oriented controlled release rate (%) of QTP and QFCs from NSPs in PBS containing 5 U/mL esterase (n = 3). QD was ultimately released into the media from QDN after 1 to 3 days and then rapidly converted to QTP by esterase. The concentration of QD was below the detection limit after 24 h. Meanwhile, QMN showed a sustained drug release profile in the esterase-added environment, with 80% QM released and converted to QTP in 4 weeks in a controlled manner (Figure 9A). In contrast, the release rate of QTP from QSN was much slower as compared to QDN and QMN, with less than 5% of QTP released after 1 week. The slow conversion rate from QS to QTP could contribute to a very slow QTP release pattern. The concentration of QS released was relatively high even on the first day and remained unchanged from the 1st to the 4th week of this experiment (Figure 9B). The diffusion of QS from the dialysis tube to the release media was deterred by the saturation of QS in the medium (the sink condition was not achieved).
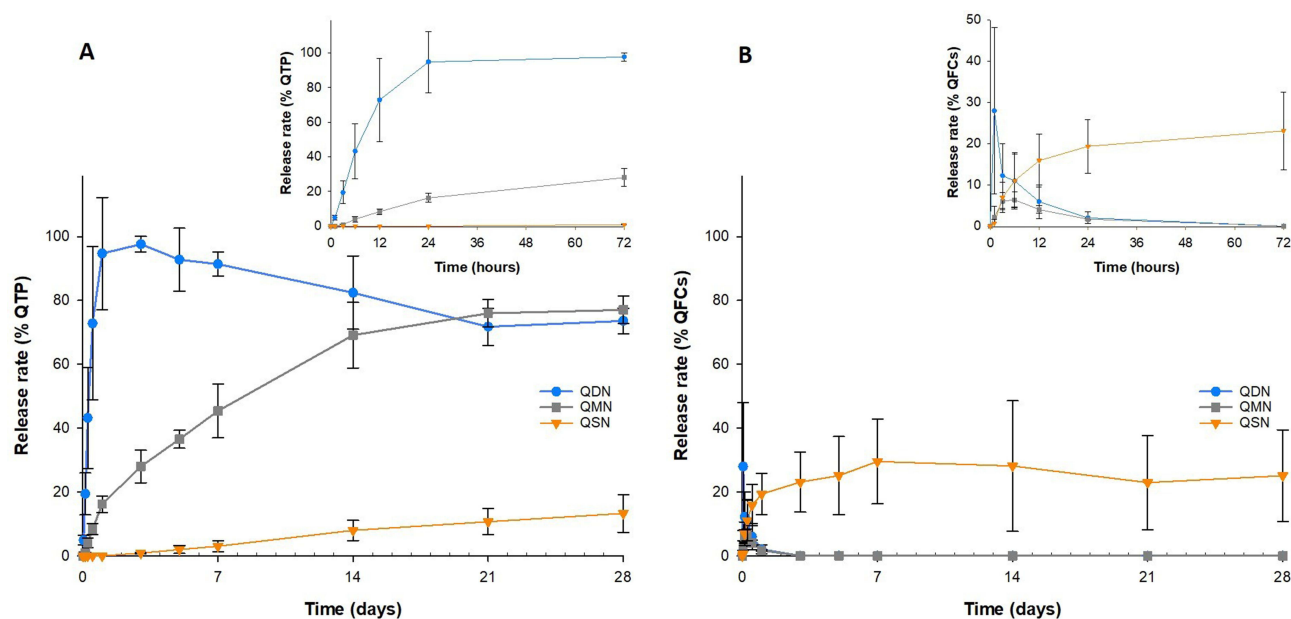

Figure 9 Enzyme-oriented controlled release rate (%) of quetiapine (**A**) and quetiapine-fatty acid conjugate (**B**) from nanosuspension powder in PBS containing 5 U/mL esterase (n=3).

These results demonstrated that the bioconversion rate to QTP of QFCs significantly affected the drug release profile of nanosuspension. However, drug release profiles of QDN or QSN having both larger initial burst release (QDN) or slower delayed pattern (QSN) were undesirable in terms of therapeutic effectiveness and long-term treatment. For this reason, QMN was optimally chosen as a potential enzyme-oriented controlled release system to develop a LAI formulation of QTP. This novel and simple pH-triggering self-assembled NSPs in low pH was easily prepared and then freeze-dried to turn free-flowing and long-acting injectable nanosuspension powders without using polymers, surfactants and high-shear mechanical operations such as milling or grinding for particle size reduction utilized in various top-down methods. To the best of our knowledge, there are no commercial products or previous studies related to long-acting nanosuspension formulations of QTP pioneered by fattigation platform, namely fatty acid conjugation to drug and macromolecules.

Conclusions

We synthesized and investigated three QFCs by varying the chain length of saturated fatty acids (C10, C14, and C18). The difference in carbon chain length impacted the physicochemical properties of the three conjugates, including solubility and the conversion rate to QTP in the human plasma or liver fraction. Under acidic environment, QFCs could be protonated and behave as amphiphilic chemical structures with CMC values depending on the fatty acid chain length. In addition, the conjugate concentration or proton-to-quetiapine ratio greatly impacted the pH-triggering NP formation. As a result, at pH 1.2, these conjugates could self-assemble to form free-flowing injectable NSPs. The fatty acid carbon chain length also contributed to the difference in particle size, stability, and drug release profile among three injectable NSPs. Among the three NSPs, QMN having C14 showed enzyme-oriented controlled QTP release over 1 month in the esterase-added environment and could be suitable as a LAI dosage form for QTP. This new and simple pH-triggering self-assembly method can also be applicable to prepare LAI NSPs of antipsychotic drugs and other rare disease drugs with pH-dependent solubility using the fattigation platform.

Abbreviations

QTP, Quetiapine; QFC, Quetiapine-fatty acid conjugate; QD, Quetiapine decanoate; QM, Quetiapine myristate; QS, Quetiapine stearate; NP, Nanoparticle; NSP, nanosuspension; QDN, Quetiapine decanoate nanosuspension; QMN, Quetiapine myristate nanosuspension; QSN, Quetiapine stearate nanosuspension; LAI, Long-acting injectable; FT-IR, Fourier transform infrared spectroscopy; NMR, Nuclear magnetic resonance; MALDI-TOF-MS, Matrix-assisted laser desorption/ionization time-of-flight mass spectroscopy; DLS, Dynamic light scattering; PDI, Polydispersity index; SEM, Scanning electron microscope; FE-TEM, Field emission transmission electron microscope; HPLC, High-performance liquid chromatography.

Data Sharing Statement

The data presented in this study are available upon request.

Acknowledgments

Author Contributions

All authors made a significant contribution to the work reported, whether that is in the conception, study design, execution, acquisition of data, analysis and interpretation, or in all these areas; took part in drafting, revising or critically reviewing the article; gave final approval of the version to be published; have agreed on the journal to which the article has been submitted; and agree to be accountable for all aspects of the work.

Disclosure

The authors declare that they have no known competing financial interests or personal relationships that could have influenced the work reported in this paper.

References

1. Sun SX, Liu GG, Christensen DB, Fu AZ. Review and analysis of hospitalization costs associated with antipsychotic nonadherence in the treatment of schizophrenia in the United States. *Curr Med Res Opin*. 2007;23(10):2305–2312. doi:10.1185/030079907X226050

2. Park EJ, Amatya S, Kim MS, et al. Long-acting injectable formulations of antipsychotic drugs for the treatment of schizophrenia. *Arch Pharmacal Res*. 2013;36(6):651–659. doi:10.1007/s12272-013-0105-7

3. Shi Y, Lu A, Wang X, Belhadj Z, Wang J, Zhang Q. A review of existing strategies for designing long-acting parenteral formulations: focus on underlying mechanisms, and future perspectives. *Acta Pharmaceutica Sinica B*. 2021;11(8):2396–2415. doi:10.1016/j.apsb.2021.05.002

4. Meyer J. Understanding depot antipsychotics: an illustrated guide to kinetics. *CNS Spectr*. 2013;18(s1):55–68. doi:10.1017/S1092852913000783

5. Darville N, van Heerden M, Vynckier A, et al. Intramuscular administration of paliperidone palmitate extended-release injectable microsuspension induces a subclinical inflammatory reaction modulating the pharmacokinetics in rats. *J Pharma Sci*. 2014;103(7):2072–2087. doi:10.1002/jps.24014

6. Ravindran AV, Al-Subaie A, Abraham G. Quetiapine: novel uses in the treatment of depressive and anxiety disorders. *Expert Opinion Invest Drug*. 2010;19(10):1187–1204. doi:10.1517/13543784.2010.515586

7. Asmal L, Flegar SJ, Wang J, Rummel-Kluge C, Komossa K, Leucht S. Quetiapine versus other atypical antipsychotics for schizophrenia. *Cochrane Database Syst Rev*. 2013:111.

8. Sweetman SC. Martindale: the complete drug reference; 2005.

9. Shetab Boushehri MA, Dietrich D, Lamprecht A. Nanotechnology as a platform for the development of injectable parenteral formulations: a comprehensive review of the know-hows and state of the art. *Pharmaceutics*. 2020;12(6):510. doi:10.3390/pharmaceutics12060510

10. Jain R, Meyer J, Wehr A, Rege B, von Moltke L, Weiden PJ. Size matters: the importance of particle size in a newly developed injectable formulation for the treatment of schizophrenia. *CNS Spectr*. 2020;25(3):323–330. doi:10.1017/S1092852919000816

11. Vo CL-N, Park C, Lee B-J. Current trends and future perspectives of solid dispersions containing poorly water-soluble drugs. *Eur J Pharm Biopharm*. 2013;85(3, Part B):799–813. doi:10.1016/j.ejpb.2013.09.007

12. Kipp JE. The role of solid nanoparticle technology in the parenteral delivery of poorly water-soluble drugs. *Int J Pharm*. 2004;284(1):109–122. doi:10.1016/j.ijpharm.2004.07.019

13. Tran TT-D, Tran PH-L, Yoon T-J, Lee B-J. Fattigation-platform theranostic nanoparticles for cancer therapy. *Mater Sci Eng C*. 2017;75:1161–1167. doi:10.1016/j.msec.2017.03.012

14. Ngo HV, Bak HE, Nguyen HD, Lee KW, Park C, Lee BJ. Physicochemical and biopharmaceutical controllability of new self-assembled fatty acid conjugated leuprolide for the enhanced anticancer activity. *Int J Nanomed*. 2023;18:2325–2344. doi:10.2147/IJN.S401048

15. Park J, Ngo H, Jin H-E, Lee K, Lee B-J. Hydroxyl group-targeted conjugate and its self-assembled nanoparticle of peptide drug: effect of degree of saturation of fatty acids and modification of physicochemical properties. *Int J Nanomed*. 2022;17:2243–2260. doi:10.2147/IJN.S356804

16. Meyer JM. Converting oral to long-acting injectable antipsychotics: a guide for the perplexed. *CNS Spectr*. 2017;22(S1):14–28. doi:10.1017/S1092852917000840

17. Ogawa N, Kaga M, Endo T, et al. Quetiapine free base complexed with cyclodextrins to improve solubility for parenteral use. *Chem Pharm Bull*. 2013;61(8):809–815. doi:10.1248/cpb.c13-00157

18. Hilaire JR, Bade AN, Sillman B, et al. Creation of a long-acting rilpivirine prodrug nanoformulation. *J Control Release*. 2019;311–312:201–211. doi:10.1016/j.jconrel.2019.09.001

19. Huttunen KM. Identification of human, rat and mouse hydrolyzing enzymes bioconverting amino acid ester prodrug of ketoprofen. *Bioorg Chem*. 2018;81:494–503. doi:10.1016/j.bioorg.2018.09.018

20. Barltrop JA, Owen TC, Cory AH, Cory JG. 5-(3-carboxymethoxyphenyl)-2-(4,5-dimethylthiazolyl)-3-(4-sulfophenyl)tetrazolium, inner salt (MTS) and related analogs of 3-(4,5-dimethylthiazolyl)-2,5-diphenyltetrazolium bromide (MTT) reducing to purple water-soluble formazans As cell-viability indicators. *Bioorg Med Chem Lett*. 1991;1(11):611–614.

21. Ngo VH, Park C, Tran TTD, Nguyen VH, Lee B-J. Mechanistic understanding of salt-induced drug encapsulation in nanosuspension via acid-base neutralization as a nanonization platform technology to enhance dissolution rate of pH-dependent poorly water-soluble drugs. *Eur J Pharm Biopharm*. 2020;154:8–17. doi:10.1016/j.ejpb.2020.07.001

22. D'Souza S, Faraj JA, Giovagnoli S, DeLuca PP. In vitro–in vivo correlation from lactide-co-glycolide polymeric dosage forms. *Prog Biomater*. 2014;3(2–4):131–142. doi:10.1007/s40204-014-0029-4

23. Li J, Yoong SL, Goh WJ, et al. In vitro controlled release of cisplatin from gold-carbon nanobottles via cleavable linkages. *Int J Nanomed*. 2015;10:7425–7441. doi:10.2147/IJN.S93810

24. Shi L, Wu X, Li T, et al. An esterase-activatable prodrug formulated liposome strategy: potentiating the anticancer therapeutic efficacy and drug safety. *Nanoscale Adv*. 2022;4(3):952–966. doi:10.1039/D1NA00838B

25. Turra BO, Barbisan F, Azzolin VF, et al. Unmetabolized quetiapine exerts an in vitro effect on innate immune cells by modulating inflammatory response and neutrophil extracellular trap formation. *Biomed Pharmacother*. 2020;131:110497. doi:10.1016/j.biopha.2020.110497

26. FDA. Center for drug evaluation and research; 2004. Available from: https://www.accessdata.fda.gov/drugsatfda_docs/nda/2007/022047Orig1s000ChemR.pdf. Accessed June 18, 2021.

27. Johnson L, Gray DM, Niezabitowska E, McDonald TO. Multi-stimuli-responsive aggregation of nanoparticles driven by the manipulation of colloidal stability. *Nanoscale*. 2021;13(17):7879–7896. doi:10.1039/D1NR01190A

28. Inácio Â, Mesquita K, Baptista M, Ramalho-Santos J, Vaz W, Vieira O. In vitro surfactant structure-toxicity relationships: implications for surfactant use in sexually transmitted infection prophylaxis and contraception. *PLoS One*. 2011;6:e19850.

29. Sharker KK, Yusa S-I, Phan CM. Micellar formation of cationic surfactants. *Heliyon*. 2019;5(9):e02425. doi:10.1016/j.heliyon.2019.e02425

30. Lu Y, Zhang E, Yang J, Cao Z. Strategies to improve micelle stability for drug delivery. *Nano Res*. 2018;11(10):4985–4998. doi:10.1007/s12274-018-2152-3